IFN-g-induced Jmjd3-*Zeb1* axis contributes to an aggressive phenotype in lung adenocarcinoma

Jianjian Yang
Huazhong University of Science and Technology
Xue Wang
Huazhong University of Science and Technology
Bing Huang
Huazhong University of Science and Technology
Rong Liu
Huazhong University of Science and Technology
Hui Xiong
Huazhong University of Science and Technology
Fan Ye
Huazhong University of Science and Technology
Chenxi Zeng
Huazhong University of Science and Technology
Xiangning Fu
Huazhong University of Science and Technology
Lequn Li (lqli@tjh.tjmu.edu.cn)
Huazhong University of Science and Technology

Research

Keywords: IFN-□□□lung adenocarcinoma, ZEB1, JMJD3, EMT

Posted Date: September 22nd, 2020

DOI: https://doi.org/10.21203/rs.3.rs-75572/v1

Abstract

Background

Active IFN-γ signaling is a common feature of tumors responding to PD-1 checkpoint blockade. IFN-γ exhibits both anti- and pro-tumor activities. Therefore, identifying the pro-tumor effects of IFN-γ and their underlying molecular mechanisms could be a critical step for developing therapeutic strategies to maximize the anti-tumor efficacy of immunotherapies.

Methods

Western blot, immunofluorescence, and quantitative real-time PCR assays were used to evaluate the expression of ZEB1 and EMT associated biomarkers. Trans-well assay was used to examine the role of IFN-γ on cancer cell migration *in vitro*. Murine tumor xenograft models were performed to examine the effect of IFN-γ on cancer cell metastasis *in vivo*. Colony formation assay was performed to detect the role of ZEB1 in cell proliferation. RNA-seq was performed to analyze the EMT-associated gene expression patterns in response to IFN-g treatment. Loss-of-function analysis and chromatin immunoprecipitation were used to reveal the mechanism underlying ZEB1 induction by IFN-γ.

Results

we demonstrate that the treatment of lung adenocarcinoma cells with IFN-γ leads to a rapid increase of ZEB1 expression and a significant change in epithelial-mesenchymal-transition (EMT)-associated gene expression patterns. Moreover, functional analysis shows that IFN-γ promotes cell migration *in vitro* and metastasis *in vivo*. Mechanistically, IFN-γ-induced JMJD3 significantly reduces H3K27 trimethylation in the promoter of the *ZEB1* gene, thereby activating *ZEB1* transcription. Inhibition of JMJD3 abrogates IFN-γ-induced ZEB1 expression. We previously demonstrated that IFN-γ-mediated anti-tumor response, including suppression of cell proliferation and induction of CXCL9 and CXCL10 expression, is STAT1-IRF1 dependent. The knockdown of *ZEB1* diminishes IFN-γ-mediated cell migration and metastasis, but it does not affect STAT1 and IRF1 expression and has no effect on cell proliferation as well as the induction of CXCL9 and CXCL10 expression.

Conclusion

Inhibition or downregulation of ZEB1 may prevent the pro-tumor activity of IFN-γ while retaining its anti-tumor function. The study expands our understanding of IFN-γ-mediated signaling and helps to identify therapeutic targets to improve current immunotherapies.

Background

The inhibition of PD1/PD-L1 has led to a paradigm shift in the treatment of lung adenocarcinoma. Important consequences of PD1/PD-L1 blockade are increased T cell function and IFN-γ production [1]. IFN-γ is one of the most important cytokines in anti-tumor immunity and immunotherapies. IFN-γ has direct tumor cell-specific anti-tumor effects, such as cell cycle arrest and the subsequent inhibition of lung cancer cell proliferation [2]. Garris and coworkers have demonstrated that effective anti-PD-1 cancer immunotherapy requires T cell–dendritic cell crosstalk and involves the cytokines IFN-γ and IL-12 [3]. Genomic defects in the IFN-γ pathway in tumor cells, including mutations in both IFN-γ receptors, JAK2, and the IFN-γ signaling downstream protein IRF1, contribute to resistance to immunotherapy [4–6]. IFN-γ promotes CXCL9, CXCL10, and CXCL11 expression, thereby increasing the recruitment of $CXCR3^+$ T cells into the tumor microenvironment, which plays a crucial role in determining the effectiveness of immunotherapy [7, 8].

Despite the pivotal role of IFN-γ in anti-tumor host immunity, under certain circumstances, IFN-γ induces tumor progression [9]. IFN-γ, like most cytokines, induces inhibitory feedback mechanisms to restrain the magnitude of the immune response [1]. For instance, the high concentration of IFN-γ produced by functional cytolytic T cells induces PD-L1 expression, which enables tumor cells to acquire the capability to counterattack immune cells [10, 11]. In fact, sustained IFN signaling in tumor cells triggers STAT1-dependent epigenetic and transcriptional changes, which consequently lead to the expression of multiple ligands for T-cell inhibitory receptors besides PD-1/PD-L1, which in turn confers tumor resistance to PD-1/PD-L1-based immunotherapy [12]. Moreover, very recently, IFN-γ has been reported to induce epithelial-mesenchymal-transition (EMT) in prostate cancer and renal cancer and to stimulate metastasis. In these cases, IFN-γ regulates the turnover of specific tumor-suppressive microRNAs, such as miR-363 in particular, through the upregulation of the IFN-stimulated gene IFN-induced tetratricopeptide repeat 5 (*IFIT5*), consequently leads to EMT in cancer cells [13]

EMT has long been associated with the acquisition of malignant cell traits, such as motility and invasiveness [14]. EMT is executed by EMT activating transcription factors (EMT-TFs), mainly of the SNAIL, TWIST, and ZEB families [15]. These transcription factors, in addition to activating classical EMT-associated events, play important roles in cancer initiation, cancer cell plasticity, and cancer progression [16, 17]. It remains unclear whether IFN-γ induces EMT-TF expression and promotes EMT in lung adenocarcinoma cells. In this study, we demonstrated that IFN-γ is capable of inducing ZEB1 expression and promoting EMT in lung cancer cells. Mechanistic analysis revealed that IFN-γ stimulation results in upregulation of JMJD3, decreased trimethylation of lysine 27 of the histone H3 subunit (H3K27me3) in the promoter region of *ZEB1*, and consequently increased ZEB1 expression. Knockdown of *ZEB1* in lung adenocarcinoma cells eliminates IFN-γ-mediated pro-tumor effects while retaining its anti-tumor functions.

Methods

Cell lines and cell culture

Human lung adenocarcinoma A549, HCC827, H1975, H2228, H1573, H2444, and UMC-11 cell lines were obtained from Cobioer Biosciences (Nanjing, China). Short tandem repeat analysis was performed for all of the cell lines. Lung adenocarcinoma cells were maintained as a monolayer culture in RPMI-1640 (GIBCO, Grand Island, NY) supplemented with 10% fetal bovine serum (FBS) (GIBCO, Grand Island, NY) and 1% penicillin/streptomycin (Hyclone, Logan, UT, USA).

Antibodies and reagents

All of the antibodies and reagents are listed in Table S1.

Long-term treatment with IFN-g

Cells were plated according to the experimental requirements. After complete attachment to the plate surface, indicated concentrations of IFN-g were added. Medium containing IFN-g was changed every 3 days.

RNA isolation and qRT-PCR analysis

The TRIzol method was used to isolate total RNA. TRIzol was obtained from TAKARA (Dalian, China). RNA was reverse transcribed into cDNA using the RT Reagent Kit according to the manufacturer's protocol (Vazyme Biotech Co., Ltd, China). qRT-PCR was carried out using Fast SYBR Green Master Mix (Life technologies, Carlsbad, CA, USA). The primers were obtained from TsingKe Biological Technology (Wuhan, China). The primer sequences are presented in Table S2. Negative controls without template were included, and all of the reactions were conducted in triplicate. b-Actin was used as internal control. Relative expression of target genes was determined by the $2^{-\Delta\Delta Ct}$ method.

SiRNA transfections

SiRNA sequences specifically targeting *JAK2*, *STAT1*, *ZEB1*, and *JMJD3* were synthesized by RiboBio (Guangzhou, China). Reverse transfection method was used to deliver SiRNA into cells. Briefly, SiRNA (50 nM) and Lipofectamine 3000 (Life Technologies, Carlsbad, CA, USA) were gently premixed in medium without FBS as per the guidelines. The transfection mixture was added to the culture plate and subsequently, cells were plated and maintained in culture for 24 h or 48 h. Knockdown efficacy was evaluated using RT-PCR and western blotting.

SiJAK2- GGAGTATCTTGGTACAAAA

SiSTAT1- GGAGGAATTGGAACAGAAA

SiJMJD3- GATTCTTTCTATGGGCTTT

SiZEB1-GAGCAAGTGTCTGAAGAAA

Preparation of short hairpin RNA (shRNA) and cell transfection

The shRNA sequence targeting *ZEB1* (shRNA-ZEB1) was 5'-GAACCAGTTGTAAATGTAA -3'. ShRNA-ZEB1 was inserted in the GV493 vector (hU6-MCS-CBh-gcGFP-IRES-puromycin, GeneChem, Shanghai, China). Empty GV493 vector was used as a negative control. Knockdown of *ZEB1* was confirmed by RT-PCR and western blotting.

ShZEB1- GAACCAGTTGTAAATGTAA

RNA-seq

Total RNA was isolated from cells using the RNeasy Mini Kit (Qiagen, Germany). Paired-end libraries were synthesized using the VAHTS Stranded mRNA-seq Library Prep Kit for Illumina (Vazyme) following the manufacturer's guide. Briefly, the poly-A containing mRNA molecules were purified using poly-T oligo-attached magnetic beads. Purified libraries were quantified with a Qubit® 2.0 Fluorometer (Life Technologies, Carlsbad, CA, USA) and validated with an Agilent 2100 bioanalyzer (Agilent Technologies, USA) to confirm the insert size and calculate the mole concentration. Clusters were generated by cBot with the library diluted to 10 pM and sequenced on Illumina HiSeq X-ten (Illumina, USA). Library construction and sequencing were performed at Shanghai Biotechnology Corporation. The RNA-seq data have been deposited in the Gene Expression Omnibus database under accession code GSE150255.

Western blotting

Cells were lysed and proteins were separated by SDS-PAGE and transferred to Immobilon-P membranes (Millipore, Germany). The blots were developed using the ECL detection system (Advansta, USA). To ensure that equal amounts of sample protein were applied per lane, b-Actin was used as loading control.

Histone extraction

Cells were harvested and washed twice with ice-cold PBS. Subsequently, cells were resuspended in Triton Extraction Buffer (TEB: PBS containing 0.5% Triton X-100 and 2 mM PMSF) at a cell density of 10^7 cells/ml. Then the cells were lysed on ice for 10 min with gentle stirring, and centrifuged at 400 *g* for 10 min at 4°C. The cell pellet was resuspended in 0.2N HCl at a cell density of 4×10^7 cells/ml at 4°C overnight. The samples were centrifuged at 400 *g* for 10 min at 4°C, and the supernatant was used for immunoblot analysis.

Immunofluorescence staining of cultured cells and mouse lung sections

Cells cultured on cover slides were pretreated with indicated reagents for 72 h. The cells were fixed with 4% paraformaldehyde for 20 min, permeabilized with 0.1% Triton X-100 for 10 min, blocked with 5% BSA for 0.5 h and labeled with primary antibody at 4°C overnight. The cells were staining with secondary antibody for 0.5 h at room temperature, and cells were counterstained with DAPI for 10 min at room temperature. Cells were visualized with a fluorescence microscope (Olympus, Tokyo, Japan).

Cell proliferation assay

Cell proliferation was assessed using the CCK-8 Kit (Dojindo Molecular Laboratories, Kumamoto, Japan). Cells were seeded (3,000–5,000 in 100μl/well) and cultured overnight before exposure to the indicated stimuli. Absorbance was measured at 450 nm using a microplate spectrophotometer (TECAN).

Colony-forming assay

Cells were seeded in 6-well plates at a density of 800 cells /well and maintained for 14 days with or without IFN-g (100 IU/ml). The cells were fixed with 4% (w/v) paraformaldehyde for 20 min, stained with crystal violet for 15 min and washed with PBS three times. The stained cell colonies (with ≥ cells 50) were counted.

Transwell migration assay

The cell migration assay was carried out using 8 μm pore size Transwell chambers (Corning, NY, USA). In brief, cells were suspended in serum-free medium and plated into the upper chambers (7×10^4 cells in 100ul/well). In the lower chambers, medium supplemented with 10% FBS was used as a chemo-attractant. IFN-g and other indicated reagents were added to both chambers at equal concentrations. After 24 h of incubation, the cells that migrated through the membrane to the bottom surface were fixed with 4% (w/v) paraformaldehyde, and stained with 0.1% (w/v) crystal violet. The migratory cells were examined under an optical microscope at 200× magnification. The average numbers of migratory cells were obtained from three randomly chosen fields.

Chromatin immunoprecipitation

The ChIP assay was performed using ChIP following the manufacturer's instructions Kit (Cell Signaling Technology, Inc.). Immunoprecipitation was performed overnight at 4°C with anti-H3K27me3 and anti-H3K4me3 antibodies, and normal rabbit IgG control. The fragments of the human *ZEB1* promoter in immunoprecipitates were identified by qPCR. Detailed information on primers is provided in Supplemental Table 2.

Animal model

NCG mice were purchased from the Experimental Animal Center (Hubei, China) and maintained in an environment with a standardized barrier system (System Barrier Environment No.00021082). A549 cells, A549-shRNA-control cells, and A549-shRNA-ZEB1 cells pretreated with IFN-g (400 IU/ml) for 4 days or without IFN-g treatment were resuspended in 100 ml PBS and then injected into the tail vein of NCG mice (2×10^6 cells/mouse), followed by i.p. injection of IFN-g (2000 IU in 100ul per mouse) every other day for total three times. Histologically detectable lung metastatic foci were observed microscopically 7 days post-injection [18]. The lungs were excised, fixed in 10% formalin, paraffin-embedded and stained with hematoxylin and eosin (H&E) for pathological identification of tumor nodules in the lung parenchyma. The photomicrographs of the lungs were taken using a light microscope (Axio Observer 3, Zeiss, Germany). The metastasis area and lung area were quantified using ImageJ software.

Ex vivo culture of patient-derived lung cancer explants

Fresh lung cancer tissues were obtained from patients undergoing pulmonary resection prior to radiation or chemotherapy in the Department of Thoracic Surgery, Tongji Hospital. The *ex vivo* culture was performed as previously described [19]. Briefly, fresh human lung cancer tissue was dissected into 1 mm^3 cubes, placed on a Gelatin sponge (HuSHiDa, Jiangxi, China), and bathed in RPMI-1640 medium supplemented with 10% heat-inactivated FBS and 100 IU/ml penicillin–streptomycin. In addition, indicated amounts of IFN-g were added to the media. Tissues were cultured at 37°C for 24–36 h and collected for RNA extraction. The use of human tissue samples was approved by the Institutional Ethics Committee of the Huazhong University of Science and Technology.

Statistical analysis

Data in bar graphs are displayed as mean ± SD. Data between two groups were compared with the two-tailed Student *t*-test (* $P<0.05$, ** $P<0.01$, *** $P<0.001$), and one-way ANOVA test was used to compare data between three or more groups. Statistical analysis was performed with GraphPad Prism software v. 8.0. For RNA-seq data, the *P*-value significance threshold in multiple tests was set by the false discovery rate (FDR). Fold-changes were also estimated according to the FPKM in each sample. The differentially expressed genes were selected using the following criteria: FDR ≤ 0.05 and $\log_2$ (fold-change) ≥ 0.5.

Results

IFN-γ induces ZEB1 expression in lung adenocarcinoma.

Previously, we performed a global transcriptome study (microarray analysis) and compared tumor tissues with high versus low *IFNG* expression level. *ZEB1* mRNA levels were significantly higher in tumors with high *IFNG* expression (GSE99995). To determine whether IFN-γ has the ability to induce *ZEB1* transcription in lung cancer cells, five lung adenocarcinoma cell lines and the lung carcinoid cell line UMC-11 were cultured with IFN-γ, and *ZEB1* mRNA levels were evaluated. Significantly higher *ZEB1* mRNA levels were observed in all five lung adenocarcinoma cell lines cocultured with IFN-γ, whereas IFN-γ appeared to have no effect on *ZEB1* expression in lung carcinoid cells (Fig. 1a). Immunoblotting analysis revealed that ZEB1 protein levels increased within 12 h upon IFN-γ stimulation and sustained for at least 72 h after a single treatment (Fig. 1b). Strikingly, prolonged exposure of A549 and H1975 cells to IFN-γ led to sustained ZEB1 expression even after removal of IFN-γ (Fig. 1c).

Furthermore, we cultured human-derived lung adenocarcinoma cells with IFN-γ *ex vivo*. IFN-γ was able to induce *ZEB1* transcription (Fig. 1d). Interestingly, exogenous IFN-γ did not significantly increase *ZEB1* mRNA levels in distant non-tumor lung tissues from patients with lung cancer (Fig. 1e). Our data demonstrate that IFN-γ induces ZEB1 expression at both mRNA and protein levels in lung adenocarcinoma cells.

IFN-γ induces EMT in lung adenocarcinoma cells.

E-cadherin and Vimentin are the most commonly used EMT markers, as their expression patterns undergo dramatic changes during EMT. In A549, HCC827, and H2228 lung cancer cells, IFN-γ stimulation downregulated E-cadherin expression and upregulated Vimentin expression, as determined by immunoblot analysis (Fig. 2a). The altered expression patterns of E-cadherin and Vimentin in lung cancer cells upon IFN-γ treatment were further validated by immunofluorescence analysis (Fig. 2b). Real-time PCT (RT-PCR) analysis revealed that *CDH1* transcription was decreased at 24 h and maintained at a low level in A549 and H2228 cells, whereas *VIM* transcription was significantly increased to various degrees in the three cell lines in response to IFN-γ stimulation (Fig. 2c).

Treatment with low amounts of IFN-γ (10 IU/ml) for 3 days did not significantly affect E-cadherin levels in A549 and HCC827 (Supplementary Fig. 1a). While treatment with IFN-γ at 25 IU/ml significantly downregulated E-cadherin levels in A549 and HCC827 cells (Supplementary Fig. 1b). Interestingly, prolonged exposure to IFN-γ induced morphological changes in A549 and HCC827 cells, which acquired a fibroblast-like appearance (Fig. 2c). The fibroblast-like appearance of A549 cells became even more evident after treatment with IFN-γ for 21 days (Supplementary Fig. 1c), indicating that IFN-γ–treated cells enter a stable mesenchymal-associated state. Substantial evidence has shown that EMT is associated with increased cell migration *in vitro*. As shown in Fig. 2e, the migratory capability of A549 and HCC827 cells was indeed significantly increased after IFN-γ treatment. IFN-γ treatment led to increases in migration of 57% and 45% in A549 and HCC827 cells, respectively. Collectively, these data demonstrate that IFN-γ induces EMT in lung adenocarcinoma cells and promotes cell migration *in vitro*.

IFN-γ-induced ZEB1 expression stimulates EMT.

EMT involves a robust reprogramming of gene expression. We analyzed the transcriptome alternations by RNA-seq analysis during EMT following IFN-γ treatment. It has been reported that A549 cells have mesenchymal characteristics, whereas HCC827 cells have epithelial features [20]. For these reasons, we selected A549 and HCC827 cells to investigate the reprogramming of gene transcription by IFN-γ. An EMT signature consisting of 130 genes was analyzed, including 67 upregulated mesenchymal-associated genes and 63 downregulated epithelial-associated genes (Supplementary Table 3) [21]. Of the 63 epithelial-associated genes, 35 genes including *CDH1*, were highly expressed in HCC827 cells compared with A549 cells; of the 67 mesenchymal-associated genes, 35 genes, including *VIM*, were expressed at lower levels in HCC827 cells than in A549 cells (Fig. 3a). These results indicate that relative to A549 cells, HCC827 cells have more epithelial-associated features, which was consistent with the reports by others [20]. EMT is a dynamic process with intermediary states that is not easily identified in cultured cells. We performed transcriptome analysis after the cells were treated with IFN-γ for 8 or 24 h. The number of differentially expressed genes was dramatically increased after 24 h of stimulation with IFN-γ compared with 8 h of stimulation (Supplementary Fig. 2A).

In A549 cells, 58 genes were differentially expressed after 24 h of IFN-γ treatment, including 20 upregulated and 38 downregulated genes ($Log_2FC \geq 0.5$, $P < 0.05$) (Fig. 3b and Supplementary Table 4). Among these differentially expressed genes, of 67 genes that are upregulated in EMT, 13 genes were

upregulated after IFN-γ treatment, and of 63 genes that are downregulated in EMT, 23 genes were downregulated after IFN-γ treatment. In HCC827 cells, 58 genes were differentially expressed after 24 h of IFN-γ treatment, including 32 upregulated and 26 downregulated genes ($Log_2FC \geq 0.5$, $P < 0.05$) (Fig. 3c and Supplementary Table 5); among these differentially expressed genes, of 67 genes that upregulated in EMT, 21 genes were upregulated after IFN-γ treatment, and of 63 genes that are downregulated in EMT, 12 genes were downregulated after IFN-γ treatment. Detailed analysis revealed that IFN-γ stimulation of the mesenchymal-like A549 cells led to downregulation of more epithelial-associated genes (genes downregulated during EMT) whereas IFN-γ stimulation of the epithelial-like HCC827 cells led to upregulation of more mesenchymal-associated genes (genes upregulated during EMT). Although IFN-γ altered the expression patterns of E-cadherin and Vimentin in both A549 and HCC827 cells, transcriptome analysis of EMT-associated genes in IFN-γ-treated cells revealed that IFN-γ induced EMT in lung cancer cells is not a unified state. The characteristics of IFN-γ-induced EMT could be associated with the intrinsic state of untreated lung cancer cells.

Although IFN-γ differentially alters the expression of EMT-associated genes in A549 and HCC827 cells, RNA-seq analysis showed that the expression of 15 genes was equally affected in both cell lines upon IFN-γ treatment, including 7 upregulated and 8 downregulated genes. Among the upregulated genes, *CTGF*, which encodes connective tissue growth factor (CTGF), is able to induce EMT and its expression levels are highly correlated with EMT markers [22]. *FGF2*, which encodes basic fibroblast growth factor, and *MAP1B*, which encodes a protein belonging to the microtubule-associated protein family, are both upregulated during EMT [21]. FGF2 promotes EMT and metastasis through the FGFR1–ERK1/2–SOX2 axis in FGFR1-amplified lung cancer [23]. Actin binding LIM protein 1, encoded by *ABL1M1* gene, plays multiple roles in establishing and maintaining cellular structure through mediating interactions between actin filaments and cytoplasmic LIM binding partners [24]. *ABLIM1* is downregulated during EMT [21]. These differentially expressed genes in response to IFN-γ stimulation in both A549 and HCC827 cells were confirmed by quantitative RT-PCR (Fig. 3d).

RNA-seq analysis revealed that *ZEB1* but not Snail and Slug was significantly upregulated in both A549 and HCC827 cells as early as 8 h upon IFN-γ stimulation (Supplementary Fig. 2A). The effect of IFN-g on the expression of Snail and Slug was confirmed by quantitative RT-PCR (Supplementary Fig. 2B). To determine whether ZEB1 is involved in IFN-γ induced EMT, we knocked down *ZEB1* using small interfering RNA (siRNA) in lung cancer cells (Supplementary Fig. 3a). Knockdown of *ZEB1* abrogated the IFN-γ-induced upregulation of *VIM* transcription (Fig. 3e). IFN-γ-mediated alterations in the expression patterns of E-cadherin and Vimentin in A549 and HCC827 cells were reversed upon *ZEB1* knockdown (Fig. 3f).

ZEB1 is required for IFN-γ-promoted cell migration and metastasis.

To determine whether ZEB1 is required for IFN-γ-promoted cell migration, we used siRNA-ZEB1 to knock down *ZEB1* (Supplementary Fig. 3a). The migratory capability of A549 cells promoted by IFN-γ was significantly compromised by the downregulation of ZEB1 expression (Fig. 4a). To examine the *in vivo* effects of IFN-γ on lung cancer cell metastasis, we established an *in vivo* metastasis model by

intravenous injection of A549 cells that had been treated with IFN-γ *in vitro* for 4 days into NCG mice (2×10^6 cells/mouse) (Fig. 4b). The mice were given recombinant human IFN-γ (2000 IU/mouse) intraperitoneally (i.p.) every other day for total three times. Seven days after injection of A549 cells, lung tissues were collected and the presence of metastatic foci and the size of metastases were analyzed microscopically. Control mice were given untreated A549 cells and the mice were not given IFN-γ. As shown in Fig. 4c, IFN-γ treatment significantly increased the number and the size of metastatic nodules in lung tissues.

To determine the role of ZEB1 in this event, we transfected A549 cells with short hairpin RNA against *ZEB1* (shRNA-ZEB1) and obtained a stable *ZEB1*-depleted cell line (Supplementary Fig. 3b). The IFN-γ-promoted increase of A549 cell migration *in vitro* was diminished in shRNA-ZEB1 A549 cells (Fig. 4d). Our *in vivo* metastasis model showed that the number and the size of metastatic nodules were reduced in mice injected with IFN-γ-treated shRNA-ZEB1 A549 cells compared with mice injected with IFN-γ-treated control A549 cells, indicating that loss of *ZEB1* dramatically reduces IFN-γ-promoted metastasis of A549 cells (Fig. 4e). Our data demonstrate that ZEB1 is responsible for IFN-γ-induced cell migration *in vitro* and metastasis *in vivo*.

JAK2-STAT1-dependent upregulation of JMJD3 enhances ZEB1 transcription via demethylation of H3K27.

We next evaluated whether IFN-γ-induced activation of the JAK2–STAT1 pathway is involved in regulation of ZEB1 expression. IFN-γ–treated JAK2–deficient H1573 cells did not exhibit altered expression levels of E-cadherin or *ZEB1* (Supplementary Figs. 3c and d), suggesting that IFN-γ–induced EMT and upregulation of *ZEB1* might be dependent on JAK2–mediated signaling. To confirm this, we knocked down *JAK2* by siRNA-JAK2 in A549 and HCC827 cells (Supplementary Fig. 3e). These cells were subsequently stimulated with IFN-γ. Upregulation of ZEB1 by IFN-γ was no longer observed (Fig. 5a). We used the same approach to determine whether STAT1 is required for IFN-γ–induced ZEB1 expression (Supplementary Fig. 3f). As shown in Fig. 5b, IFN-γ–induced ZEB1 expression was diminished in cells transfected with siRNA-STAT1, indicating that IFN-γ–induced ZEB1 expression requires JAK2–STAT1.

ZEB1 transcription is regulated by the modulation of the chromatin environment at gene regulatory elements [25, 26]. H3K27me3 is often associated with transcriptional repression. The relative absence of H3K27me3 in the chromatin at the *ZEB1* promoter signals active transcription [25]. Interestingly, the expression of H3K27 trimethylation and the ratio of H3K27me3 to H3 were rapidly reduced in A549 cells after exposure to IFN-γ (Figs. 5c and d). JMJD3, a direct transcriptional target of STAT1, catalyzes the demethylation of H3K27me3 [27]. For these reasons, we examined whether IFN-γ induces JMJD3 expression. *JMJD3* transcription was rapidly upregulated in A549 and HCC827 cells upon exposure to IFN-γ (Fig. 5e). Immunoblot analysis revealed increased JMJD3 expression after 3 h of IFN-γ treatment (Fig. 5f). To determine whether JMJD3 is associated with IFN-γ-induced ZEB1 expression, the JMJD3 specific inhibitor GSK-J4 was used [28]. GSK-J4 significantly reduced IFN-γ stimulated increasing in *ZEB1* mRNA levels (Fig. 5g) and protein levels (Fig. 5h). Knockdown experiments with siRNA-JMJD3 further

confirmed that IFN-γ-induced ZEB1 expression requires JMJD3 (Supplementary Fig. 3g and Fig. 5i). Downregulation of STAT1 expression led to abrogation of IFN-γ-induced JMJD3 expression (Fig. 5j), confirming that IFN-γ-induced JMJD3 expression is STAT1–dependent.

Since H3K27 demethylation is linked to transcriptional activation, we examined whether H3K27 demethylation is associated with the transcription of *ZEB1*. The *ZEB1* promoter exhibits a bivalent chromatin configuration [28]. H3K4me3 is associated with transcriptional initiation [29], whereas the H3K27me3 is associated with transcriptional repression. We performed a chromatin immunoprecipitation (ChIP) assay at the *ZEB1* promoter to compare the levels of histone modifications in control versus IFN-γ–treated cells. IFN-γ treatment led to a significant reduction in H3K27me3 levels at the *ZEB1* promoter in A549 cells, whereas IFN-γ did not significantly affect H3K4me3 levels at the *ZEB1* promoter (Fig. 5k). These data demonstrate that IFN-γ enables the *ZEB1* promoter to transition from the bivalent to the active chromatin state, at least in part through the demethylation of H3K27me3.

IFN-γ regulates PD-L1 expression via miR-200–ZEB1 axis.

ZEB1 transcription is tightly regulated by microRNA. Recent studies have revealed that IFN-γ promotes *ZEB1* expression through IFIT5-mediated suppression of miR-363 in prostate cancer and renal cancer [13]. We did not observe downregulation of *miR-363* expression by IFN-γ in lung cancer cells (Supplementary Fig. 4). It is well known that the *miR-200* family inhibits *ZEB1* expression and plays a major role in preventing ZEB1 from triggering EMT. In turn, ZEB1 can directly repress the transcription of *miR-200* loci [30]. As shown in Fig. 6a, *miR-200c* expression was significantly reduced in A549 and HCC827 cells after 12 h of IFN-γ treatment, and the reduction of *miR-200c* expression was even more dramatic after 24 and 48 h of IFN-γ treatment. We wondered whether IFN-γ–promoted *ZEB1* expression in lung cancer cells is related to the downregulation of *miR-200* expression. IFN-γ-induced upregulation of *ZEB1* transcription was observed after 4 h in both A549 and HCC827 cells, whereas *miR-200c* expression was not affected even after 6 h of IFN-γ stimulation (Figs. 6b and c). Our data suggest that IFN-γ first promotes *ZEB1* transcription, and subsequently suppresses *miR-200c* expression.

PD-L1 expression has been reported to be directly regulated by *miR-200* family members [31]. We examined whether IFN-γ–induced PD-L1 expression can be regulated by ZEB1. Knockdown of *ZEB1* by siRNA did indeed lead to a significant reduction of IFN-γ-induced PD-L1 expression in A549 and HCC827 cells (Fig. 6d). Further analysis revealed that downregulation of *ZEB1* enhanced *miR-200* expression (Fig. 6e). Our data indicate that IFN-γ stimulation rapidly induces ZEB1 expression and consequently downregulates *miR-200c*, which at least partially contributes to the upregulation of PD-L1 expression.

IFN-γ–mediated anti–proliferation and induction of CXCL9 and CXCL10 expression are not affected by ZEB1 knockdown.

Previous studies by us and others have shown that IFN-γ suppresses the proliferation of lung cancer cells [2, 32]. We wondered whether ZEB1 is involved in IFN-γ-mediated suppression of cell proliferation. The JMJID3 inhibitor GSK-J4 revered IFN-γ-induced ZEB1 expression (Figs. 5g and h). However, GSK-J4 did

not affect IFN-γ-mediated suppression of A549 cell proliferation (Fig. 7a). Knockdown of *ZEB1* by siRNA did not alter the anti-proliferative effects of IFN-γ in both A549 and HCC827 cells (Fig. 7b). *ZEB1* knockdown had no significant effect on IFN-γ-mediated suppression of colony formation (Fig. 7c). Cyclin E1, which is encoded by the *CCNE1* gene, plays a critical role in the control of cell cycle progression by allowing G1 to S phase transition [33]. IFN-γ-treated A549 cells exhibited significantly lower *CCNE1* mRNA levels than untreated A549 cells (Fig. 7d). Knockdown of *ZEB1* had no effect on the IFN-γ-mediated reduction of *CCNE1* expression (Fig. 7d). A previous study by us has shown that IFN-γ-mediated suppression of cell proliferation requires STAT1 and IRF1 [2]. Downregulation of *ZEB1* had no effect on IFN-γ-induced STAT1 and IRF1 expression at mRNA and protein levels (Figs. 7e and f). *ZEB1* knockdown did not affect IFN-γ-induced phosphorylation of STAT1 (Fig. 7g). Additionally, *CXCL9* and *CXCL10*, which encodes two chemokines that are important for the recruitment of activated lymphocytes to tumors, are also target genes of STAT1-IRF1. As shown in Fig. 7h, knockdown of *ZEB1* did not alter the IFN-γ-induced expression pattern of *CXCL9* and *CXCL10*.

Based on our results, we proposed a functional mechanism as shown in Fig. 7i. IFN-γ stimulation results in the rapid upregulation of the expression of the STAT1 target gene *JMJD3*, which consequently leads to the demethylation of H3K27me3 near the *ZEB1* promoter, enabling the transition from the bivalent to an active chromatin state. This leads to increased *ZEB1* transcription and protein levels. Elevated ZEB1 expression mediates IFN-γ-induced EMT and cell migration *in vitro* and promotes metastasis *in vivo*. *ZEB1* knockdown abrogates the pro-tumor effects of IFN-γ, including the induction of EMT, enhanced cell migration and upregulated PD-L1 expression, while retaining IFN-γ–activated STAT1–IRF1–mediated anti-tumor functions.

Discussion

The main findings of this study are summarized as follows. (1) IFN-γ induces EMT in lung adenocarcinoma cells. RNA-seq analysis revealed that IFN-γ stimulation altered the expression pattern of EMT-associated genes. Morphological changes in lung adenocarcinoma cells were observed after prolonged exposure to IFN-γ. Functionally, IFN-γ promoted cell migration and metastasis *in vivo*. (2) IFN-γ stimulation resulted in upregulation of JMJD3 and hence decreased H3K27 trimethylation in the promoter region of *ZEB1*, increasing ZEB1 expression. (3) Increased ZEB1 expression mediated IFN-γ-induced EMT. (4) Knockdown of *ZEB1* abrogated IFN-γ-induced EMT and PD-L1 expression. (5) Inhibition or downregulation of ZEB1 had no effect on IFN-γ-mediated anti-tumor effects, including its suppression of cell proliferation and the increase in CXCL9 and CXCL10 expression, which promotes the recruitment of T cells to the tumor microenvironment. Based on our findings, we propose that IFN-γ-induced upregulation of ZEB1 might increase the aggressiveness of lung cancer cells. Targeting ZEB1 eliminates the pro-tumor effects of IFN-γ while retaining its anti-tumor functions.

Our results showed that IFN-γ stimulation induced a dramatic change in the expression pattern of E-cadherin and Vimentin in lung cancer cells. It is widely recognized that experimental models using only a small selection of epithelial and mesenchymal biomarkers, including E-cadherin, N-cadherin and

Vimentin, to define or confirm EMT sketch an oversimplified view of this complex process. EMT is not one clearly defined tumor state but a set of multiple dynamic transitional states between epithelial and mesenchymal phenotypes [16, 34]. Due to the complexity of the EMT process, reliable biomarkers are still lacking and a comprehensive method to identify and/or measure EMT, particular *in vivo*, does not exist. Nevertheless, numerous gene expression studies have been conducted to obtain transcriptome signatures and marker genes associated with EMT [20, 35]. In our study, we not only analyzed *CDH1* and *VIM* expression levels, but we also performed a transcriptome analysis to determine whether IFN-γ alters the expression of other EMT-associated genes. We obtained the EMT core gene signatures, which consists of 130 genes, through meta-analysis of 18 independent and published gene expression studies of EMT [21]. Comparing the expression levels of these 130 genes, we found that IFN-γ stimulation altered the transcription of almost 50% of EMT-associated genes in both A549 and HCC827 cells. Among these differentially expressed genes, the EMT-associated transcription factor ZEB1 was rapidly upregulated in response to IFN-γ stimulation. In addition to these genetic biomarkers, several *in vitro* criteria have been used to determine EMT, including a spindle-shape morphology and increased migratory capability [36, 37]. We found that exposure of lung cancer cells to IFN-γ induced morphologic changes, and also promoted cell migration *in vitro* and metastasis *in vivo*. Our findings demonstrate that IFN-γ is capable of inducing EMT in lung adenocarcinoma cells.

In prostate cancer and renal cancer, IFN-γ induces EMT through the IFIT5–XRN1 complex, which regulates the turnover of specific tumor-suppressive microRNAs, such as miR-101, miR-128, and miR-363[13]. In our study, IFN-γ treatment even upregulated *miR-363* levels in lung cancer cells. Our findings suggest that the mechanism by which IFN-γ induces EMT is cancer type-dependent and context-specific. In lung cancer cells, IFN-γ stimulation led to a rapid increase in mRNA and protein levels of the STAT1-target gene *JMJD3*. In mammary epithelial cells, JMJD3 mediates TGF-β induced EMT through upregulation of *SNAIL* expression, leading to breast cancer invasion [38]. JMJD3 upregulates Slug and promotes cell migration, invasion, and transition towards a stem-like phenotype in hepatocellular carcinoma [39]. JMJD3 could be a key regulator of cancer aggressiveness. We found that targeting JMJD3 with the inhibitor GSK-J4 or JMJD3 knockdown using siRNA abrogated IFN-γ-induced ZEB1 expression.

Recently obtained evidence has indicated that EMT-associated transcription factors regulate large set of cancer cell features, extending beyond tumor migration, invasion, and metastasis. Recent studies have demonstrated a robust correlation between EMT score, ZEB1/miR-200 levels and PD-L1 expression in multiple cancer datasets [31]. In the present study we showed that IFN-γ-induced ZEB1 expression is involved in the upregulation of PD-L1 expression through its suppressive effects on *miR-200* expression. Moreover, Lou and colleagues have reported that an EMT-related mRNA signature is in fact associated with increased expression of diverse immune inhibitory ligands and receptors in lung adenocarcinoma, including PD-L1, TIM-3, LAG3 and CTLA-4 [40]. As illustrated in our working model, IFN-γ is able to simultaneously induce EMT-like features and PD-L1 expression in lung cancer cells via the upregulation of ZEB1 expression. However, whether these two events are independent remains to be elucidated. Our

findings suggest that strong anti-tumor immune properties might be accompanied by increased tumor progression through multiple means.

In this study, we found that *ZEB1* knockdown diminished IFN-γ-induced PD-L1 expression, cell migration, and metastasis. Interestingly, downregulation of ZEB1 did not affect IFN-γ-mediated suppression of cell proliferation and increased expression of *CXCL9* and *CXCL10*. JMJD3 inhibitor GSK-J4 suppressed IFN-γ-induced ZEB1 expression. GSK-J4 has been applied in the treatment of several cancers, such as acute myeloid leukemia and prostate cancer [41, 42]. Our study sheds light on the functional mechanism by which targeting ZEB1 might limit the pro-tumor effects of IFN-γ. As IFN-γ has been proven to play a critical role in PD1/PD-L1 blockage-based immunotherapies, targeting ZEB1 combined with immune checkpoint blockade might improve the anti-tumor efficacy of immunotherapies.

Conclusions

IFN-γ increases ZEB1 expression in a STAT1-JMJD3 dependent manner and consequently promotes cancer cell aggressiveness. This study provides a potential target to minimize the pro-cancer effect of IFN-γ while preserving its antitumor function.

Abbreviations

IFN-g
Interferon gamma
JMJD3
Jumonji domain containing-3
ZEB1
Zinc finger E-box binding homeobox 1
EMT
Epithelial-to-mesenchymal transition
RNA-seq
RNA sequencing
PCR
Polymerase chain reaction
shRNA
short hairpin RNA
siRNA
small interfering RNA
CHIP
Chromatin immunoprecipitation
CXCL9
C-X-C motif chemokine ligand 9
CXCL10

C-X-C motif chemokine ligand 10

JAK

Janus Kinase

STAT1

Signal transducer and activator of transcription 1

IRF1

Interferon regulatory factor 1

PD-L1

Programmed death-ligand 1

Declarations

Ethics approval and consent to participate

The present study was approved by the Ethics Committee of Tongji Hospital of Huazhong University of Science and Technology. Animal experiment was approved by the Animal Care and Use Committee at Tongji Hospital, Huazhong University of Science and Technology.

Consent for publication

Not applicable.

Availability of data and materials

The analyzed datasets generated during the current study are available from the corresponding author on reasonable request.

Competing Interests

The authors declare no competing interests.

Funding

This work was supported by the National Natural Science Foundation of China (Grant numbers 81874168, 81672808, and 81472652 for L.L.).

Authors' contributions

LL and XF designed and directed the project. JY planned and carried out the majority of the experiments and supervised the experiments. XW, BH, RL, HX, FY, and CZ contributed to the experiments. All authors

provided critical feedback and helped shape the research and analysis. LL and JY took the lead in writing the manuscript with input from all authors.

Acknowledgements

Not applicable.

References

1. Ivashkiv LB. IFNgamma: signalling, epigenetics and roles in immunity, metabolism, disease and cancer immunotherapy. Nat Rev Immunol. 2018;18(9):545–58.
2. Gao Y, Yang J, Cai Y, Fu S, Zhang N, Fu X, Li L. IFN-gamma-mediated inhibition of lung cancer correlates with PD-L1 expression and is regulated by PI3K-AKT signaling. Int J Cancer. 2018;143(4):931–43.
3. Garris CS, Arlauckas SP, Kohler RH, Trefny MP, Garren S, Piot C, Engblom C, Pfirschke C, Siwicki M, Gungabeesoon J, et al. Successful Anti-PD-1 Cancer Immunotherapy Requires T Cell-Dendritic Cell Crosstalk Involving the Cytokines IFN-gamma and IL-12. Immunity. 2018;49(6):1148–61 e1147.
4. Gao J, Shi LZ, Zhao H, Chen J, Xiong L, He Q, Chen T, Roszik J, Bernatchez C, Woodman SE, et al. Loss of IFN-gamma Pathway Genes in Tumor Cells as a Mechanism of Resistance to Anti-CTLA-4 Therapy. Cell. 2016;167(2):397–404. e399.
5. Zaretsky JM, Garcia-Diaz A, Shin DS, Escuin-Ordinas H, Hugo W, Hu-Lieskovan S, Torrejon DY, Abril-Rodriguez G, Sandoval S, Barthly L, et al. Mutations Associated with Acquired Resistance to PD-1 Blockade in Melanoma. N Engl J Med. 2016;375(9):819–29.
6. Shin DS, Zaretsky JM, Escuin-Ordinas H, Garcia-Diaz A, Hu-Lieskovan S, Kalbasi A, Grasso CS, Hugo W, Sandoval S, Torrejon DY, et al. Primary Resistance to PD-1 Blockade Mediated by JAK1/2 Mutations. Cancer Discov. 2017;7(2):188–201.
7. Chow MT, Ozga AJ, Servis RL, Frederick DT, Lo JA, Fisher DE, Freeman GJ, Boland GM, Luster AD. Intratumoral Activity of the CXCR3 Chemokine System Is Required for the Efficacy of Anti-PD-1 Therapy. Immunity. 2019;50(6):1498–512 e1495.
8. Han X, Wang Y, Sun J, Tan T, Cai X, Lin P, Tan Y, Zheng B, Wang B, Wang J, et al. Role of CXCR3 signaling in response to anti-PD-1 therapy. EBioMedicine. 2019;48:169–77.
9. Mandai M, Hamanishi J, Abiko K, Matsumura N, Baba T, Konishi I. Dual Faces of IFNgamma in Cancer Progression: A Role of PD-L1 Induction in the Determination of Pro- and Antitumor Immunity. Clin Cancer Res. 2016;22(10):2329–34.
10. Minn AJ, Wherry EJ. Combination Cancer Therapies with Immune Checkpoint Blockade: Convergence on Interferon Signaling. Cell. 2016;165(2):272–5.
11. Bellucci R, Martin A, Bommarito D, Wang K, Hansen SH, Freeman GJ, Ritz J. Interferon-gamma-induced activation of JAK1 and JAK2 suppresses tumor cell susceptibility to NK cells through

upregulation of PD-L1 expression. Oncoimmunology. 2015;4(6):e1008824.

12. Benci JL, Xu B, Qiu Y, Wu TJ, Dada H, Twyman-Saint Victor C, Cucolo L, Lee DSM, Pauken KE, Huang AC, et al. Tumor Interferon Signaling Regulates a Multigenic Resistance Program to Immune Checkpoint Blockade. Cell. 2016;167(6):1540–54 e1512.
13. Lo UG, Pong RC, Yang D, Gandee L, Hernandez E, Dang A, Lin CJ, Santoyo J, Ma S, Sonavane R, et al. IFNgamma-Induced IFIT5 Promotes Epithelial-to-Mesenchymal Transition in Prostate Cancer via miRNA Processing. Cancer Res. 2019;79(6):1098–112.
14. Chaffer CL, San Juan BP, Lim E, Weinberg RA. EMT, cell plasticity and metastasis. Cancer Metastasis Rev. 2016;35(4):645–54.
15. Goossens S, Vandamme N, Van Vlierberghe P, Berx G. EMT transcription factors in cancer development re-evaluated: Beyond EMT and MET. Biochim Biophys Acta Rev Cancer. 2017;1868(2):584–91.
16. Nieto MA, Huang RY, Jackson RA, Thiery JP. Emt: 2016. Cell. 2016;166(1):21–45.
17. De Craene B, Berx G. Regulatory networks defining EMT during cancer initiation and progression. Nat Rev Cancer. 2013;13(2):97–110.
18. Karagiannis GS, Pastoriza JM, Wang Y, Harney AS, Entenberg D, Pignatelli J, Sharma VP, Xue EA, Cheng E, D'Alfonso TM, et al: **Neoadjuvant chemotherapy induces breast cancer metastasis through a TMEM-mediated mechanism**. *Sci Transl Med* 2017, 9(397).
19. Ravindranathan P, Lee TK, Yang L, Centenera MM, Butler L, Tilley WD, Hsieh JT, Ahn JM, Raj GV. Peptidomimetic targeting of critical androgen receptor-coregulator interactions in prostate cancer. Nat Commun. 2013;4:1923.
20. Byers LA, Diao L, Wang J, Saintigny P, Girard L, Peyton M, Shen L, Fan Y, Giri U, Tumula PK, et al. An epithelial-mesenchymal transition gene signature predicts resistance to EGFR and PI3K inhibitors and identifies Axl as a therapeutic target for overcoming EGFR inhibitor resistance. Clin Cancer Res. 2013;19(1):279–90.
21. Groger CJ, Grubinger M, Waldhor T, Vierlinger K, Mikulits W. Meta-analysis of gene expression signatures defining the epithelial to mesenchymal transition during cancer progression. PLoS One. 2012;7(12):e51136.
22. Zhu X, Zhong J, Zhao Z, Sheng J, Wang J, Liu J, Cui K, Chang J, Zhao H, Wong S. Epithelial derived CTGF promotes breast tumor progression via inducing EMT and collagen I fibers deposition. Oncotarget. 2015;6(28):25320–38.
23. Wang K, Ji W, Yu Y, Li Z, Niu X, Xia W, Lu S. FGFR1-ERK1/2-SOX2 axis promotes cell proliferation, epithelial-mesenchymal transition, and metastasis in FGFR1-amplified lung cancer. Oncogene. 2018;37(39):5340–54.
24. Roof DJ, Hayes A, Adamian M, Chishti AH, Li T. Molecular characterization of abLIM, a novel actin-binding and double zinc finger protein. J Cell Biol. 1997;138(3):575–88.
25. Chaffer CL, Marjanovic ND, Lee T, Bell G, Kleer CG, Reinhardt F, D'Alessio AC, Young RA, Weinberg RA. Poised chromatin at the ZEB1 promoter enables breast cancer cell plasticity and enhances

tumorigenicity. Cell. 2013;154(1):61–74.

26. Gao Y, Zhao Y, Zhang J, Lu Y, Liu X, Geng P, Huang B, Zhang Y, Lu J: **The dual function of PRMT1 in modulating epithelial-mesenchymal transition and cellular senescence in breast cancer cells through regulation of ZEB1**. *Sci Rep* 2016, **6**:19874.
27. Przanowski P, Dabrowski M, Ellert-Miklaszewska A, Kloss M, Mieczkowski J, Kaza B, Ronowicz A, Hu F, Piotrowski A, Kettenmann H, et al. The signal transducers Stat1 and Stat3 and their novel target Jmjd3 drive the expression of inflammatory genes in microglia. J Mol Med (Berl). 2014;92(3):239–54.
28. Heinemann B, Nielsen JM, Hudlebusch HR, Lees MJ, Larsen DV, Boesen T, Labelle M, Gerlach LO, Birk P, Helin K. Inhibition of demethylases by GSK-J1/J4. Nature. 2014;514(7520):E1–2.
29. Guenther MG, Levine SS, Boyer LA, Jaenisch R, Young RA. A chromatin landmark and transcription initiation at most promoters in human cells. Cell. 2007;130(1):77–88.
30. Burk U, Schubert J, Wellner U, Schmalhofer O, Vincan E, Spaderna S, Brabletz T. A reciprocal repression between ZEB1 and members of the miR-200 family promotes EMT and invasion in cancer cells. EMBO Rep. 2008;9(6):582–9.
31. Chen L, Gibbons DL, Goswami S, Cortez MA, Ahn YH, Byers LA, Zhang X, Yi X, Dwyer D, Lin W, et al. Metastasis is regulated via microRNA-200/ZEB1 axis control of tumour cell PD-L1 expression and intratumoral immunosuppression. Nat Commun. 2014;5:5241.
32. Yano T, Sugio K, Yamazaki K, Kase S, Yamaguchi M, Ondo K, Sugimachi K. Direct IFNluence of interferon-gamma on proliferation and cell-surface antigen expression of non-small cell lung cancer cells. Lung Cancer. 2000;30(3):169–74.
33. Ohtsubo M, Theodoras AM, Schumacher J, Roberts JM, Pagano M. Human cyclin E, a nuclear protein essential for the G1-to-S phase transition. Mol Cell Biol. 1995;15(5):2612–24.
34. Pastushenko I, Blanpain C. EMT Transition States during Tumor Progression and Metastasis. Trends Cell Biol. 2019;29(3):212–26.
35. Tan TZ, Miow QH, Miki Y, Noda T, Mori S, Huang RY, Thiery JP. Epithelial-mesenchymal transition spectrum quantification and its efficacy in deciphering survival and drug responses of cancer patients. EMBO Mol Med. 2014;6(10):1279–93.
36. Zeisberg M, Neilson EG. Biomarkers for epithelial-mesenchymal transitions. J Clin Invest. 2009;119(6):1429–37.
37. Krebs AM, Mitschke J, Lasierra Losada M, Schmalhofer O, Boerries M, Busch H, Boettcher M, Mougiakakos D, Reichardt W, Bronsert P, et al. The EMT-activator Zeb1 is a key factor for cell plasticity and promotes metastasis in pancreatic cancer. Nat Cell Biol. 2017;19(5):518–29.
38. Ramadoss S, Chen X, Wang CY. Histone demethylase KDM6B promotes epithelial-mesenchymal transition. J Biol Chem. 2012;287(53):44508–17.
39. Tang B, Qi G, Tang F, Yuan S, Wang Z, Liang X, Li B, Yu S, Liu J, Huang Q, et al. Aberrant JMJD3 Expression Upregulates Slug to Promote Migration, Invasion, and Stem Cell-Like Behaviors in Hepatocellular Carcinoma. Cancer Res. 2016;76(22):6520–32.

40. Lou Y, Diao L, Cuentas ER, Denning WL, Chen L, Fan YH, Byers LA, Wang J, Papadimitrakopoulou VA, Behrens C, et al. Epithelial-Mesenchymal Transition Is Associated with a Distinct Tumor Microenvironment Including Elevation of Inflammatory Signals and Multiple Immune Checkpoints in Lung Adenocarcinoma. Clin Cancer Res. 2016;22(14):3630–42.
41. Li Y, Zhang M, Sheng M, Zhang P, Chen Z, Xing W, Bai J, Cheng T, Yang FC, Zhou Y. Therapeutic potential of GSK-J4, a histone demethylase KDM6B/JMJD3 inhibitor, for acute myeloid leukemia. J Cancer Res Clin Oncol. 2018;144(6):1065–77.
42. Morozov VM, Li Y, Clowers MM, Ishov AM. Inhibitor of H3K27 demethylase JMJD3/UTX GSK-J4 is a potential therapeutic option for castration resistant prostate cancer. Oncotarget. 2017;8(37):62131–42.

Figures

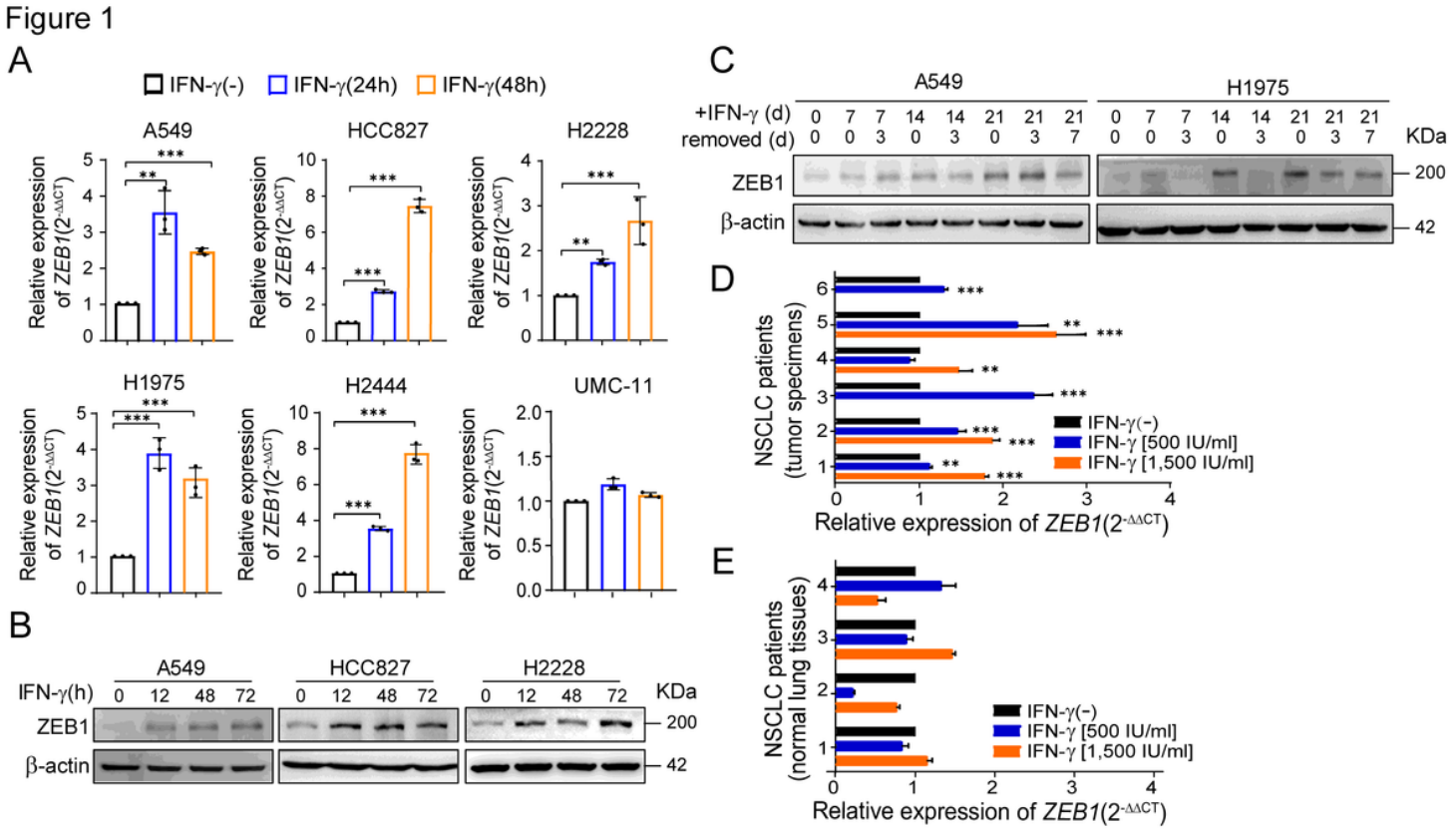

Figure 1

IFN-γregulates ZEB1 expression in lung adenocarcinoma cells. Cells were treated with or without IFN-γ (100 IU/ml) for indicated time intervals. a ZEB1 mRNA levels were quantified by RT-PCR. Data are presented as mean ± SD (n = 3) and were analyzed by the two-sided Student's t-test, *P < 0.05, **P < 0.01, *** P <0.001. b ZEB1 protein levels were analyzed by immunoblotting. Data shown are representative images of four independent experiments. c Cells were cultured with IFN-γ (25 IU/ml) for indicated time intervals. IFN-γ was removed for 3 or 7 days, and the cells were harvested and lysed. ZEB1 expression

was analyzed by immunoblotting. d Fresh human lung cancer tissue (n = 6) and (e) distant non-tumor lung tissues (> 3cm away from the edge of the tumors) (n = 4) were treated with indicated concentrations of IFN-□ for 36 h, and the tissues were collected for RNA extraction. ZEB1 mRNA levels were quantified by RT-PCR. Data are presented as mean ± SD (n = 3) and were analyzed by the two-sided Student's t-test, *P < 0.05, **P < 0.01, *** P <0.001.

Figure 2

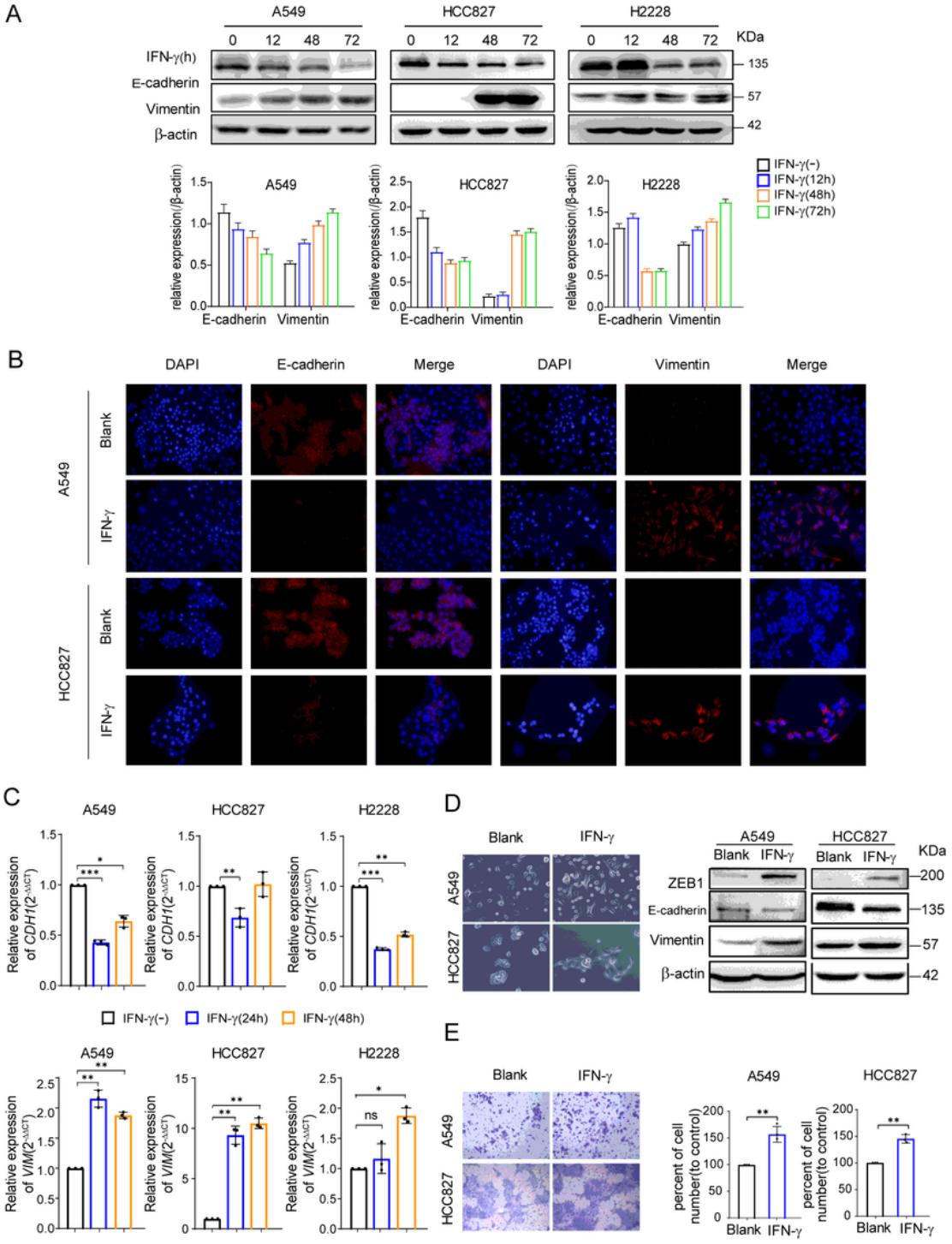

Figure 2

IFN-β induces EMT in lung adenocarcinoma cells. a Cells were cultured with or without IFN-β (100 IU/ml) for 12, 48, and 72 h, harvested, and lysed. The protein levels of E-cadherin and Vimentin were analyzed by immunoblotting. The bar graphs show densitometry analyses of changes in E-cadherin and Vimentin levels as normalized to β-actin. Data shown are representative images of four independent experiments. b Cells were treated with or without IFN-β (100 IU/ml) for 72 h, and immunostained with anti-E-cadherin (1:200) or anti-Vimentin (1:200). Blank indicates untreated cells (magnification, 200×). c Cells were treated with or without IFN-β (100 IU/ml) for 24 and 48 h. CDH1 and VIM mRNA levels were quantified by RT- PCR. Data are presented as mean ± SD (n = 3) and were analyzed by the two-sided Student's t-test, *P < 0.05, **P < 0.01, *** P <0.001, ns, not significant. d A549 and HCC827 cells were treated with or without IFN-β (25 IU/ml) for 2 weeks. Changes in cell morphology were observed by phase-contrast light microscopy (magnification, 200×). e The effects of IFN-β on cell migration were examined by Transwell assay. Cells (7×104 cells in 100 μl RPMI-1640) were suspended in serum-free medium with or without IFN-β (100 IU/ml). After 24 h, the number of cells on the bottom side of the Transwell inserts was counted in three random fields under a light microscope (magnification, 200×). Data are presented as mean ± SD and were analyzed with the two-sided Student t-test, **P < 0.01, *** P <0.001.

Figure 3

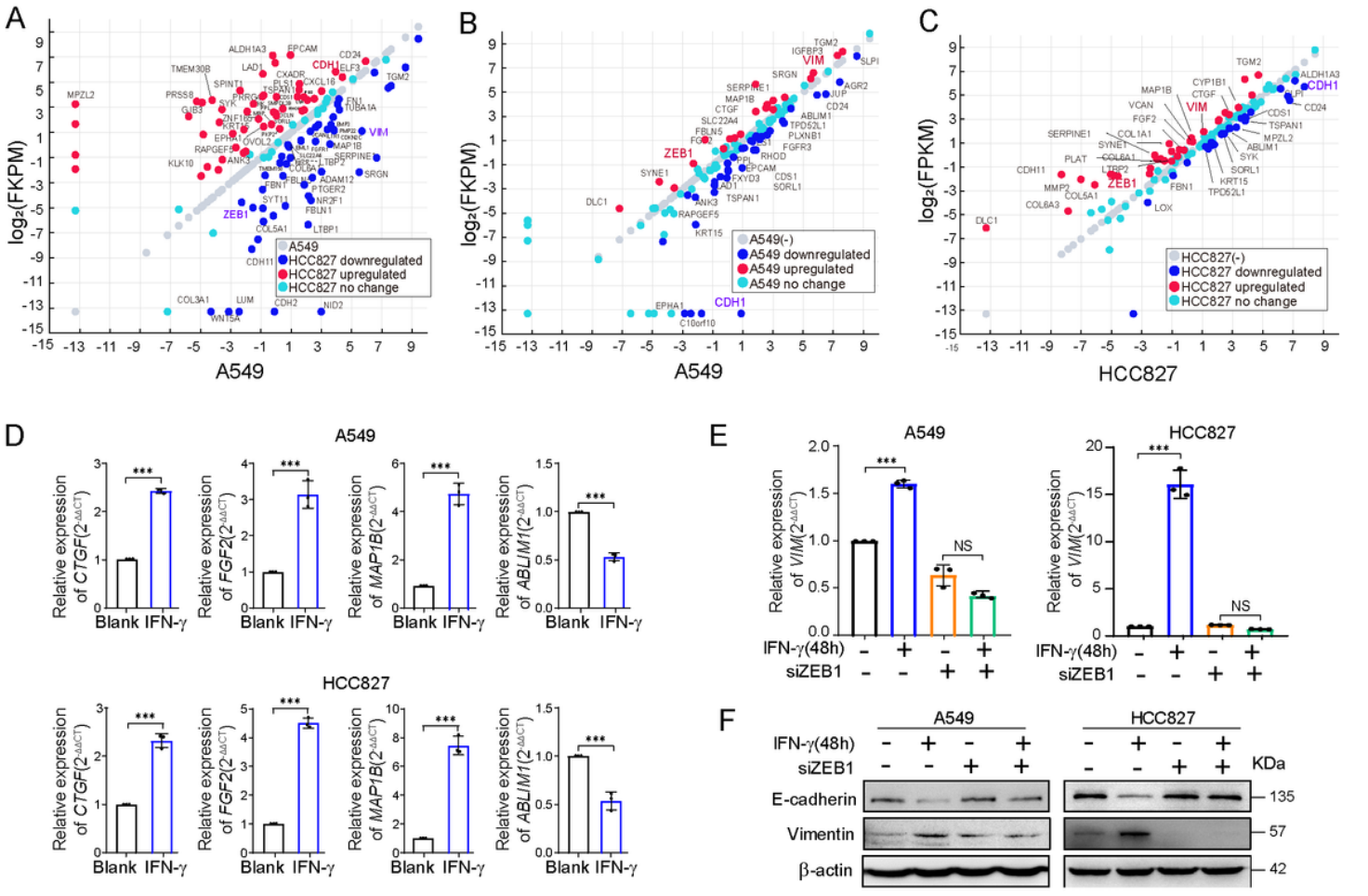

Figure 3

IFN-β-induced ZEB1 expression is responsible for EMT. Changes in the expression of EMT-associated genes in A549 and HCC827 cells are shown. a Comparison of expression profiles of EMT-associated genes between A549 and HCC827. Red dots represent EMT-associated genes upregulated in A549 cells, and blue dots indicate downregulated genes in A549 cells, and blue dots indicate genes downregulated in A549 cells, compared with HCC827 cells. Changes in the expression of EMT-associated genes in (b) A549 and (c) HCC827 cells in response to IFN-βstimulation (100 IU/ml) are shown. Red dots indicate upregulated genes and blue dots represent downregulated genes in response to IFN-βstimulation for 24 h, compared with untreated cells. d A549 and HCC827 cells were treated with IFN-β (100 IU/ml) for 24 h. The mRNA levels of CTGF, FGF2, MAP1B, and ABLIM1 were quantified by RT- PCR. Data are presented as mean ± SD (n = 3) and were analyzed with the two-sided Student's t-test, ***P <0.001. e A549 and HCC827 cells were transfected with siRNA-ZEB1 or siRNA-control for 48 h. Subsequently, the cells were suspended in medium containing 10% FBS with or without IFN-β (100 IU/ml) for 24 h. The mRNA levels of VIM were quantified by RT- PCR. Data are presented as mean ± SD (n=3) and were analyzed with one-way ANOVA, ***P < 0.001). f A549 and HCC827 cells were transfected with siRNA-ZEB1 or siRNA-control for 24 h, and the cells were suspended in medium containing 10% FBS with or without IFN-β (100 IU/ml) for 48 h. E-cadherin and Vimentin protein levels were analyzed by immunoblot.

Figure 4

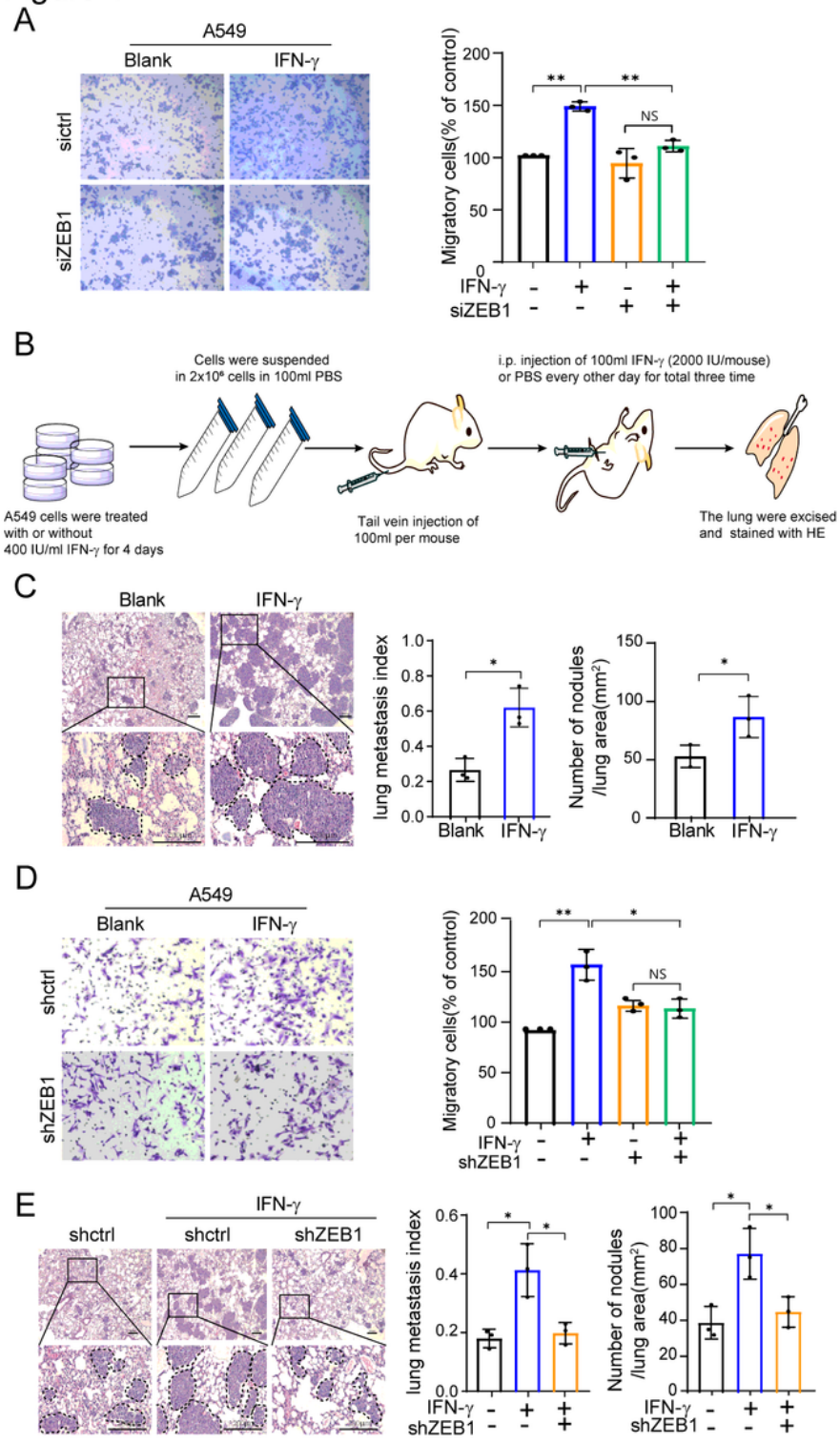

Figure 4

IFN-γ-promoted cell migration and metastasis are ZEB1-dependent. a A549 cells were transfected with siRNA-ZEB1 or siRNA-control for 48 h. Then the cells were treated with or without IFN-γ and seeded in the upper chamber for the Transwell migration assay. After 24 h, the cells in the lower chamber were counted in three random fields under a light microscope (magnification, 200×). Data are presented as mean ± SD and were analyzed with one-way ANOVA, **P < 0.01. b The establishment of an in vivo metastasis model

by intravenous injection of A549 cells into NCG mice (2 × 106 cells/mouse). c At the end of experimental period (seven days after i.v. injection of A549 cells), lung tissues were harvested and stained with hematoxylin eosin (HE). Representative images of histological inspection of mouse lungs from each group are shown (magnification, 50×; insert, 200×). The number of tumor nodules and lung metastasis index (ratio of tumor area to the total tumor and lung area) were evaluated and analyzed between IFN-□□treated and untreated groups. Data are presented as mean ± SD (n = 3) and were analyzed with the two-sided Student's t-test, * P < 0.05. Scale bar: 200 □m (d). A549 cells were transfected with shRNA-ZEB1 or shRNA-control, and a stable ZEB1 knockdown cell line was generated. Then the cells (7×104 cells in 100ul RPMI-1640) were suspended in serum-free medium with or without IFN-□□□100 IU/ml) for 24 h, the cells in the lower chamber were counted in three random fields under a light microscope (magnification, 200×). Data are presented as mean ± SD and were analyzed with one-way ANOVA, * P < 0.05, **P < 0.01, ns, not significant. e A549 cells transfected with shRNA-ZEB1 or shRNA-control were injected into NCG mice via tail vain, the animal model in (b) was used. Representative images of histological inspection of mouse lungs from each group are shown (magnification, 50×; insert, 200×). The number of tumor nodules and lung metastasis index were calculated. The tumor nodules were counted and area ratio in the lung parenchyma was calculated. Data are presented as mean ± SD (n = 3) and were analyzed one-way ANOVA, *P < 0.05.

Figure 5

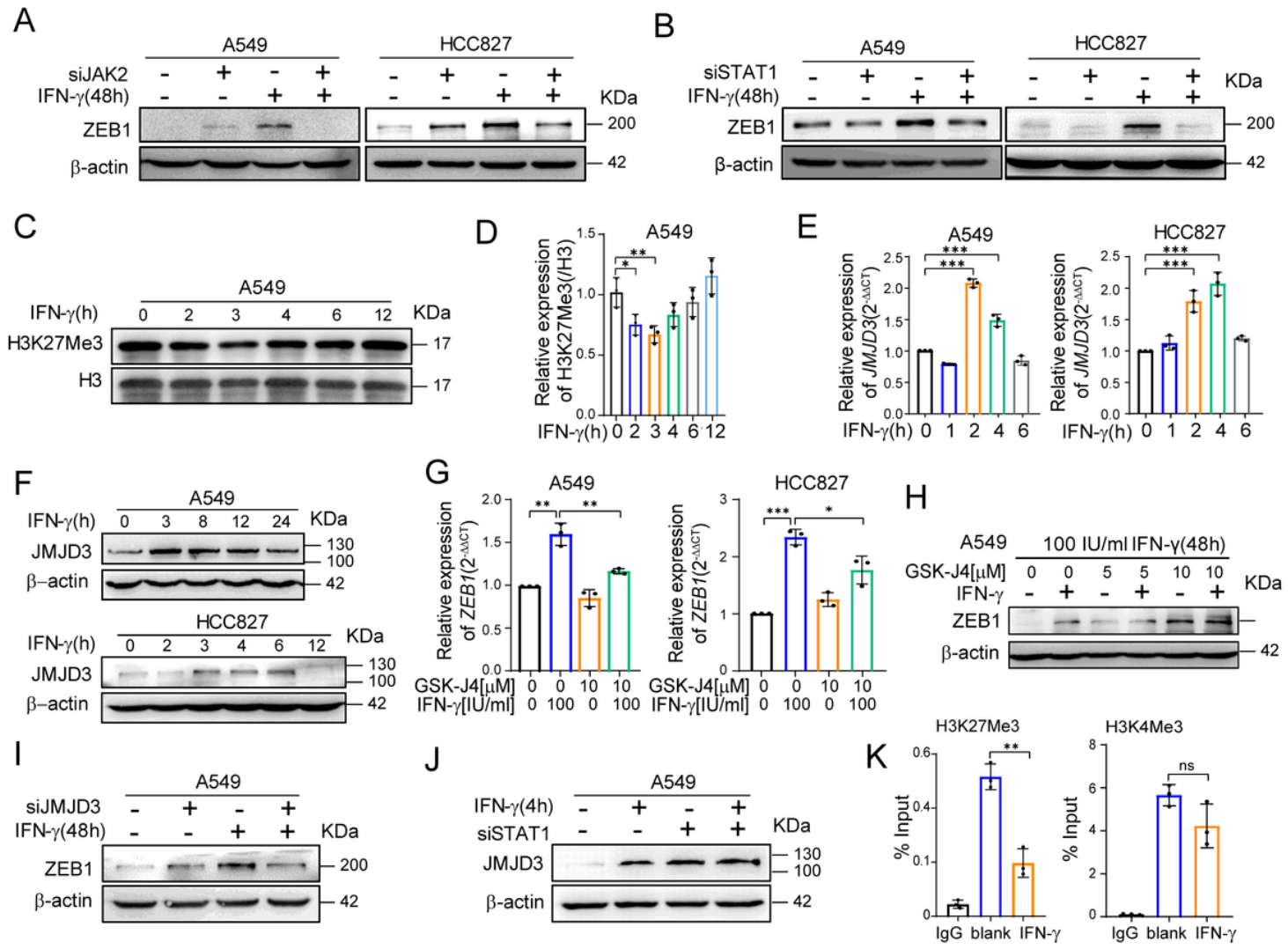

Figure 5

JAK2-STAT1 dependent upregulation of JMJD3 enhances ZEB1 transcription via demethylation of H3K27. A549 and HCC827 cells were transfected with (a) siRNA-JAK2 or (b) siRNA-STAT1 and siRNA-control for 48 h. Then the cells were cultured in medium containing 10% FBS with or without IFN-□ (100 IU/ml) for 24 h. Subsequently, ZEB1 expression was analyzed by immunoblot. A549 cells were cultured with IFN-□□for indicated time intervals, harvested, and lysed, and total histones were extracted following the Histone Extract protocol. c H3K27me3 levels were analyzed by immunoblotting. d The graph presents the quantification of H3K27me3 levels normalized to histone H3 levels. Data are presented as mean ± SD (n = 3) and were analyzed one-way ANOVA, *P < 0.05, **P < 0.01. e A549 and HCC827 cells were cultured with IFN-□ (100 IU/ml) for indicated time intervals. JMJD3 mRNA levels were quantified by RT- PCR. Untreated cells served as control. Data are presented as mean ± SD (n = 3) and were analyzed with the two-sided Student's t-test, ***P <0.001. f JMJD3 protein levels were analyzed by immunoblotting with anti-JMJD3. g Cells were cultured in medium with or without the JMJD3 inhibitor GSK-J4 (10 □M) for 1 h.

Then the cells were treated with or without IFN-β (100 IU/ml) for 8 h. ZEB1 mRNA levels were quantified by RT- PCR. Data are presented as mean ± SD (n = 3) and were analyzed with one-way ANOVA, *P < 0.05, **P < 0.01. h A549 cells were cultured in median with or without JMJD3 inhibitor GSK-J4 (5 μM or 10 μM) for 1 h. Then the cells were treated with or without IFN-β (100 IU/ml) for 48 h. ZEB1 protein levels were analyzed by immunoblotting. i A549 cells were transfected with siRNA-JMJD3 or siRNA-control for 24 h. Then the cells were treated with or without IFN-β (100 IU/ml) for 48 h. ZEB1 expression was analyzed by immunoblotting. j A549 cells were transfected with siRNA-STAT1 or siRNA-control for 48 h. Then the cells were treated with or without IFN-βββ100 IU/ml) for 4 h. JMJD3 protein levels were analyzed by immunoblotting. k A549 cells were treated with or without IFN-β for 4 h, and harvested. ChIP-qPCR was performed for H3K4me3 and H3K27me3 histone modifications at the ZEB1 promoter in A549 cells (n = 3). Data were analyzed with the two-sided Student's t-test, **P < 0.01, ns not significant.

Figure 6

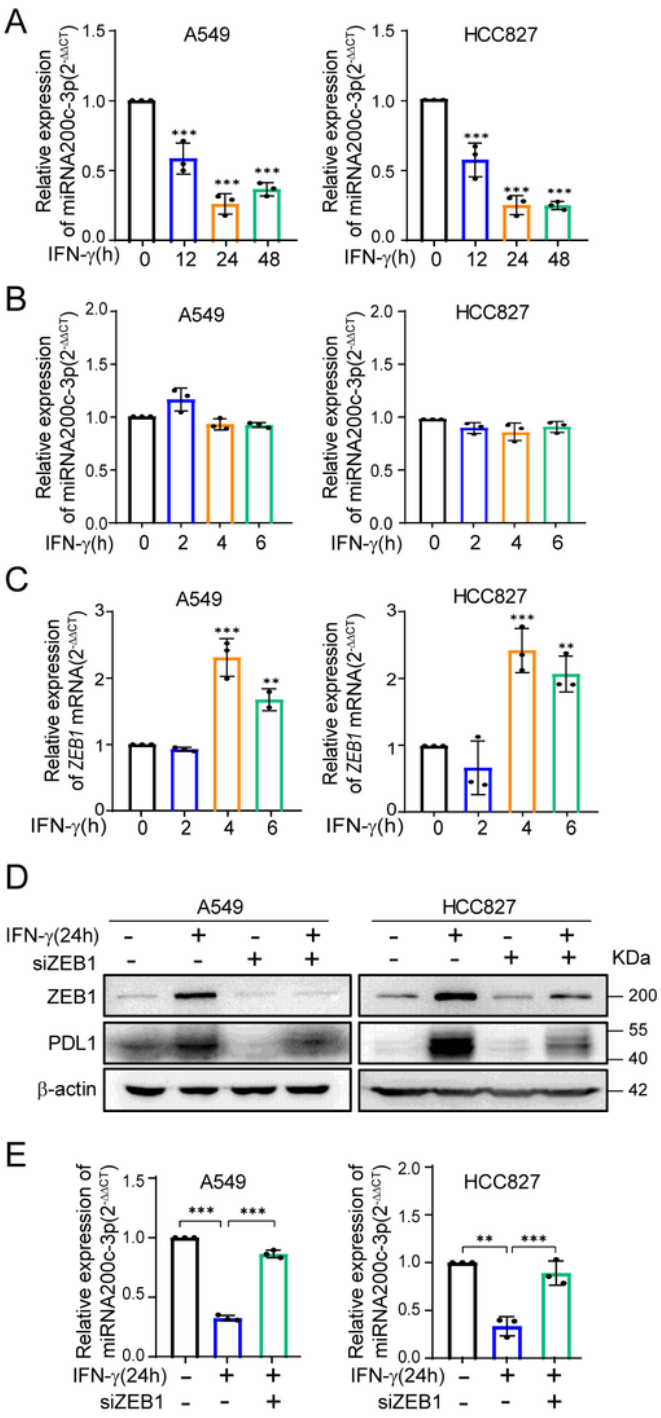

Figure 6

IFN-γ regulates the miR-200/ZEB1 axis and PD-L1 expression. A549 and HCC827 cells were cultured with IFN-γ for indicated time intervals. The levels of miR-200 (a and b) and ZEB1 mRNA (c) were quantified by RT- PCR. Data are presented as the mean ± SD (n = 3) and were analyzed with the two-sided Student's t-test, **P < 0.01. Cells were transfected with siRNA-ZEB1 or siRNA-control for 24 h. Then the cells were treated with or without IFN-γ for 48 h. d ZEB1 and PDL1 protein levels were analyzed by immunoblotting,

and (e) the levels of miR-200c-3p were quantified by RT- PCR (n = 3) and were analyzed with one-way ANOVA, **P < 0.01, ***P < 0.001.

Figure 7

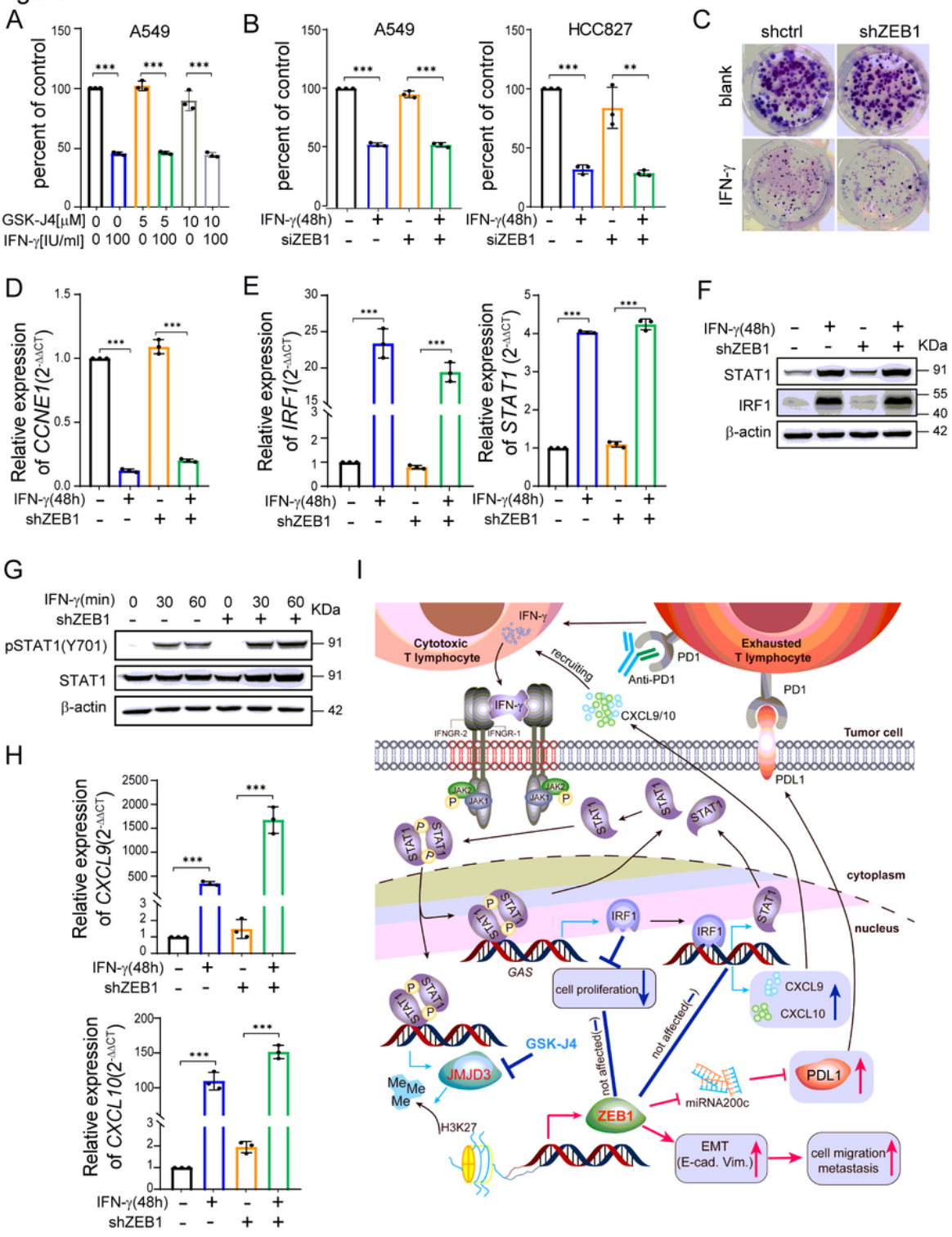

Figure 7

Downregulation of ZEB1 expression has no effect on the anti-tumor effects of IFN-□. a A549 cells (3-5×103cells/well) were cultured in medium with or without JMJD3 inhibitor GSK-J4 (5 □M or 10 □M) for 1 h. Then the cells were stimulated with or without IFN-□ (100 IU/ml) for 72 h. Proliferation was assessed

using a CCK8 kit (n = 3). Data were analyzed with one-way ANOVA. b A549 and HCC827 cells were transfected with siRNA-control or siRNA-ZEB1 for 24 h. Subsequently, the cells (5-10×103cells/well) were treated with or without IFN-□ for 48 h. Proliferation was assessed using a CCK8 kit (n = 3). Data were analyzed with one-way ANOVA. c A549-shCtrol and A549-shZEB1 cells were seeded in 6-well plates at a density of 800 cells per well and maintained for 14 days with or without IFN-□. The medium was changed every 3 days. A549-shControl and A549-shZEB1 cells were seeded in 6-well plates and cultured for 24 h. Then the cells were stimulated with or without IFN-□ (100 IU/ml) for 48 h. The mRNA levels of (d) Cyclin E and (e) STAT1 and IRF1 were quantified by RT-PCR. Data are presented as mean ± SD (n = 3) and were analyzed with one-way ANOVA. f A549-shControl and A549-shZEB1 cells were stimulated with or without IFN-□ for 24 h and harvested. STAT1 and IRF1 protein levels were analyzed by immunoblotting. g A549-shControl and A549-shZEB1 cells were stimulated with or without IFN-□ for indicated time intervals. STAT1 phosphorylation was analyzed by immunoblotting. h A549-shControl and A549-shZEB1 cells were seeded in 6-well plates for 24 h. Then the cells were stimulated with or without for 48 h. The mRNA levels of CXCL9 and CXCL10 were quantified by RT- PCR. Data are presented as the mean ± SD (n = 3) and were analyzed with one-way ANOVA, *** P < 0.001. i IFN-□ stimulation results in the rapid upregulation of the expression of the STAT1 target gene JMJD3, which consequently leads to the demethylation of H3K27me3 near the ZEB1 promoter, enabling the transition from the bivalent to an active chromatin state. This leads to increased ZEB1 transcription and protein levels. Elevated ZEB1 expression mediates IFN-□-induced EMT and cell migration in vitro and promotes metastasis in vivo. ZEB1 knockdown abrogates the pro-tumor effects of IFN-□, including the induction of EMT, enhanced cell migration and upregulated PD-L1 expression, while retaining IFN-□ activated STAT1-IRF1-mediated anti-tumor functions.

Supplementary Files

This is a list of supplementary files associated with this preprint. Click to download.

- TableS15.xlsx
- FigureS.legends.docx
- FigS4.tif
- FigS3.tif
- FigS2.tif
- FigS1.tif